

Crystal Instabilities at Finite Strain

Jinghan Wang* and Sidney Yip

Department of Nuclear Engineering, Massachusetts Institute of Technology, Cambridge, Massachusetts 02139

S. R. Phillpot and Dieter Wolf

Materials Science Division, Argonne National Laboratory, Argonne, Illinois 60439

(Received 30 August 1993)

It is demonstrated that stability criteria derived using elastic stiffness coefficients which govern stress-strain relations at finite deformation give quantitative predictions of crystal instability, as observed in direct molecular dynamics simulations. With the aid of such analysis we show that instabilities can be triggered in succession; as a consequence, the limit of metastability in the superheating of a defect-free crystal can be predicted.

PACS numbers: 62.20.Dc, 61.50.Lt, 81.40.Jj

Much of the current discussion of structural transformation driven by instabilities of a strained lattice is based on stability criteria expressed in terms of elastic constants. However, whether such criteria are or are not capable of predicting the actual onset of an instability is a question that generally has not been satisfactorily resolved. The difficulty, on the theoretical side, lies in the different ways that stability analyses have been formulated and in evaluating properly the elastic parameters which appear in them. On the experimental side, competing effects frequently render the triggering instability uncertain.

For a cubic crystal there are three generally accepted elastic stability criteria [1],

$$C_{11} + 2C_{12} > 0, \quad C_{44} > 0, \quad C_{11} - C_{12} > 0, \quad (1)$$

where C_{ij} are the conventional elastic constants (in Voigt notation). The first two have simple meanings, since the existence of bulk modulus, $B_T = (C_{11} + 2C_{12})/3$, and shear modulus, $G = C_{44}$, are obviously necessary for stability. The third criterion, the existence of a modulus against tetragonal shear, $G' = (C_{11} - C_{12})/2$, is thought to play a more subtle role which can be dominant since generally $G' < G < B_T$. In a number of long-standing problems such as melting [2], polymorphism [3], and pressure-induced amorphization [4], the criterion which is violated first is regarded as the mechanism causing the onset of the structural transformation. Because these criteria are so widely used, it is important to scrutinize their applicability to processes where the crystal is actually strained to the point of instability.

In this Letter we show that Eq. (1) is not adequate, except in the special case of zero applied stress, to describe the stability limits of perfect crystals at finite strain. Using *elastic stiffness* coefficients as the proper stress-strain relations at finite deformation, we derive generalized stability criteria as the finite-strain extensions of well-known results such as Eq. (1), normally derived using linear elasticity theory. The validity of the new criteria is demonstrated, first, in the particularly simple and illus-

trative case of instability of a perfect crystal induced by pure dilatation, by comparing the predicted critical strain against direct observation through molecular dynamics simulation. The analysis is then extended to two, more complex instabilities, one induced by uniaxial stress and the other induced by isobaric (zero pressure) heating. These results reveal that the onset of one elastic instability can trigger another in succession, an apparently general behavior which has not been fully recognized in previous studies [5-7]. This characteristic of elastic instabilities appears to be evidence for the existence of a hierarchy of crystal stability catastrophes recently suggested by Tallon [8]; as we will show below, a significant consequence is that one can thus predict the metastability limit of a superheated defect-free crystal [2,9,10].

Consider an applied uniform stress taking a crystal in an arbitrary initial configuration \mathbf{X} to a final configuration \mathbf{x} , with corresponding Lagrangian strain $\eta_{ij} = (u_{ij} + u_{ji} + u_{ij}u_{ji})/2$, where $u_{ij} = du_i/dX_j$ and $\mathbf{u} = \mathbf{x} - \mathbf{X}$. For an isothermal process the free energy change is $dF = \Omega(\mathbf{x}) \text{Tr}\{td\eta\}$, where Ω is the system volume and thermodynamic tension $t_{ij}(\mathbf{x})$ is related to the applied stress $\sigma_{ij}(\mathbf{x})$ by the transformation $t_{ij} = J_{ik}^{-1} \sigma_{kl} (J')_{lj}^{-1}$ (prime denotes transpose), with $J_{ij} = dx_i/dX_j$. The elastic stiffness, or stress-strain, coefficients will be defined as $B_{ijkl}(\mathbf{X}) \equiv [\partial \sigma_{ij}(\mathbf{x}) / \partial \eta_{kl}]_{\mathbf{X}}$; they may be written as [11,12]

$$B_{ijkl} = C_{ijkl} + \frac{1}{2} [\{\sigma_{il}(\mathbf{X}) \delta_{jk} + \sigma_{jl}(\mathbf{X}) \delta_{ik} + \sigma_{ik}(\mathbf{X}) \delta_{jl} + \sigma_{jk}(\mathbf{X}) \delta_{il}\} - 2\sigma_{ij}(\mathbf{X}) \delta_{kl}], \quad (2)$$

where $C_{ijkl} \equiv [\Omega^{-1}(\mathbf{x}) \partial^2 F(\mathbf{x}, T) / \partial \eta_{ij} \partial \eta_{kl}]_{\mathbf{X}} \equiv [\partial t_{ij}(\mathbf{x}) / \partial \eta_{kl}]_{\mathbf{X}}$ are the elastic constants evaluated at the applied stress [13]. Equation (2) shows that the stiffness coefficient tensor depends explicitly on the state of applied stress; consequently, except for isotropic or zero stress, it has different symmetry from the elastic constant tensor. The origin of the stress-dependent terms can be shown to arise from the requirement of rotational invariance of the free energy [12,14].

Stability conditions are now derived by formulating the strain energy density in terms of η_{ij} , and requiring convexity along with rotational invariance and the condition of equilibrium [12]. One finds that by expressing the strain energy as a quadratic in the strain $\delta\eta_{ij}$ and requiring the energy to be positive definite [1], one obtains stability conditions in the form of $B_{ijkl}\delta\eta_{kl} > 0$. Thus, the generalization of linear elasticity results for stability criteria to finite strain is achieved by simply replacing the elastic constants C_{ij} by the stiffness coefficients B_{ij} (Voigt notation). Because of the symmetry $B_{ijkl} = B_{jikl} = B_{jilk}$, B is a 6×6 matrix. The stability analysis becomes an eigenvalue problem leading to six instability conditions (criteria), each with an eigenmode of deformation prescribed by $\delta\eta_{ij}$ [12,15].

To clearly demonstrate the difference between Eq. (1) and the generalized stability criteria proposed here, we consider a cubic crystal under hydrostatic pressure, $\sigma_{ij} = -P\delta_{ij}$ ($P < 0$ for tension). In this case the elements of B , having the same symmetry as C , are $B_{11} = B_{22} = B_{33} = C_{11} - P$, $B_{12} = B_{21} = B_{13} = B_{31} = C_{12} + P$, and $B_{44} = B_{55} = B_{66} = C_{44} - P$. Setting $\det(B) = 0$ gives

$$\begin{aligned} M_1 &= (C_{11} + 2C_{12})/3 + P/3 > 0, \\ M_2 &= C_{44} - P > 0, \\ M_3 &= (C_{11} - C_{12})/2 - P > 0. \end{aligned} \quad (3)$$

In analogy with the corresponding criteria in Eq. (1), we will refer to the conditions in Eq. (3) as spinodal (in the sense of vanishing of B_T), shear, and Born criteria, respectively. With each of these criteria giving a critical strain η_c at which the lattice becomes unstable against that particular mode of deformation, the actual response of the system is governed by the smallest value of η_c . For pure dilatation, the eigenmodes are of the form $(1, 1, 1, 0, 0, 0)\delta\eta$, $(0, 0, 0, \delta\eta_{yz}, 0, 0)$, and $(\delta\eta_{xx}, \delta\eta_{yy}, \delta\eta_{zz}, 0, 0, 0)$ with $\delta\eta_{xx} + \delta\eta_{yy} + \delta\eta_{zz} = 0$. Thus, each instability mode can be identified by its own symmetry characteristics; in particular, we note that symmetry breaking (or "bifurcation") with volume conservation is the signature of the Born instability.

In order to obtain numerical results for the elastic stiffness coefficients as well as directly observe the crystal behavior at the point of instability, we perform molecular dynamics simulations using an interatomic potential model of the embedded-atom-method type developed for Au [16]. (The particular choice of the potential has no special significance since we are concerned only with the general nature of the results.) The simulation cell is cubic and contains $N = 504$ atoms, arranged in an fcc structure with periodic border conditions. Starting with the lattice parameter a set at the equilibrium value a_0 (corresponding to zero pressure and minimum potential energy) and temperature $T = 500$ K, we equilibrate the system at incrementally larger values while maintaining constant temperature by velocity rescaling after every time step.

The elastic stiffness coefficients are obtained through Eq. (2) and the fluctuation formulas for elastic constants [12,13]. Figure 1 shows the left-hand sides of the spinodal and Born stability criteria of Eq. (3) which lead to a prediction of the onset of instability, via the vanishing of bulk modulus, at a strain of $(a/a_0)_{th} = 1.059$. The actual instability observed by direct simulation occurs at $(a/a_0)_{obs} = 1.053$, as indicated by an abrupt release of the internal stress and a corresponding lowering of the enthalpy, both being consequences of lattice decohesion in the form of cavitation. Thus, the prediction of Eq. (3) is directly verified.

In Fig. 1 the corresponding quantities for the stability criteria of Eq. (1) are also shown; these give, in contrast, a prediction of instability, via the vanishing of tetragonal shear, at a strain of $(a/a_0)_{th} = 1.025$. Clearly then, in this case neither the nature of the instability nor the value of the critical strain are correctly predicted by Eq. (1).

To investigate the instability induced by an anisotropic external stress, we consider applying uniaxial tension, $\sigma_{ij} = -\sigma\delta_{i1}\delta_{j1}$, to an fcc lattice, where the subscript 1 denotes the x direction. The deformed system takes on tetragonal symmetry, elongating in the direction of stress and contracting in the two transverse directions. From $\det(B) = 0$ we now obtain four stability criteria,

$$(C_{22} + C_{23})(C_{11} - \sigma) - 2(C_{12} + \sigma) > 0, \quad (4)$$

$$C_{22} - C_{23} > 0, \quad C_{44} > 0, \quad C_{55} - \sigma/2 > 0,$$

with corresponding eigenmodes of deformation. These again can be identified as spinodal, Born, and two shear instabilities. Inserting the elastic constants calculated by molecular dynamics for this case, we find that the Born criterion gives the smallest value of η_c . The intersection of C_{22} and C_{23} , both increasing with a/a_0 because of

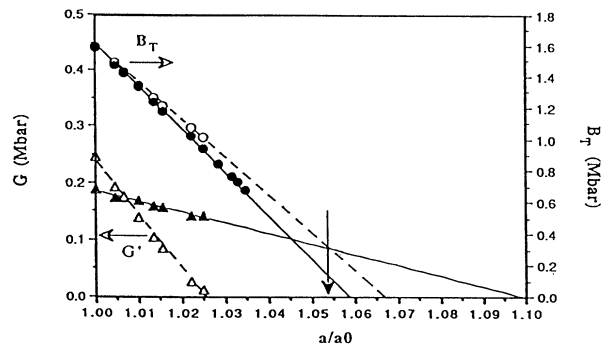


FIG. 1. Variations of M_1 (closed circles) and M_3 (closed triangles), as defined in Eq. (3), with lattice strain a/a_0 . Solid lines indicate linear extrapolations to give critical values for each instability. Also shown are B_T (open circles) and G' (open triangles) from Eq. (1) with dashed lines as linear extrapolations. Arrow indicates the critical strain observed by direct simulation.

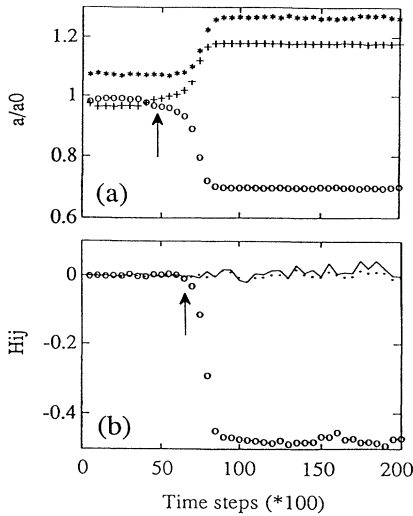


FIG. 2. Time response of (a) normalized lattice parameters along the direction of strain (asterisk) and along the two transverse directions (circle and plus), and (b) matrix elements h_{12} (circle), h_{13} (dot), and h_{23} (line). One time step is equivalent to 2×10^{-15} s.

Poisson effect, occurs at $(a/a_0)_{th} = 1.072$. This predicted value is to be compared with the observed critical strain at $(a/a_0)_{obs} = 1.073$ in a direct simulation at $T = 500$ K with $N = 108$ atoms [12].

Figure 2 shows the temporal evolution during equilibration of the lattice parameters along the three initially orthogonal directions, as well as the off-diagonal elements of the matrix h_{ij} which defines the shape of the simulation cell [5]. The above mentioned instability occurs at about time step 5000, where symmetry in the two transverse directions is broken by the system elongating in one direction while contracting in the other. Furthermore, it can be seen that a second structural response follows at time step 7000 at which point the simulation cell undergoes significant shear deformation [Fig. 2(b)]. Given the close agreement between the predicted and observed critical strains and the symmetry characteristics of the first instability, we conclude that Eq. (4) is quantitatively correct in describing the nature of the incipient instability under uniaxial strain. Although it does not necessarily follow from Eq. (4) that a second instability has to occur, nevertheless, the numerical results indicate that the next instability to occur should be a shear deformation at $a/a_0 = 1.242$. This value may be compared with the shear transformation indicated in Fig. 2(b) which is seen to occur at $a/a_0 = 1.227$. Thus there seems to be reasonably good correspondence between stability criteria and actual system response after the initial instability. In this case, the induced transition is fcc to bcc.

For the last instability to be analyzed we consider a particularly important special case of isobaric heating at zero pressure, where, according to Eq. (2), the stiffness

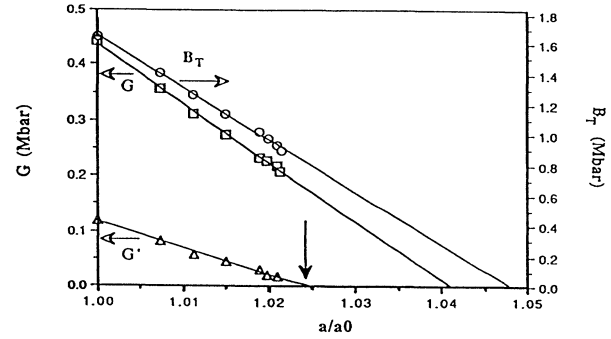


FIG. 3. Variations of B_T , G , and G' with lattice strain a/a_0 . Lines indicate linear extrapolations to give critical values for each instability. Arrow indicates the critical strain observed by direct simulation.

coefficients are equal to the elastic constants, and the stability criteria given in Eq. (1) are now valid. Using the same molecular dynamics model as before but with a larger simulation cell, $N = 1372$, we have calculated the temperature variations of the elastic constants up to 1300 K. Figure 3 shows the left-hand sides of the stability criteria of Eq. (1) after making a one-to-one correspondence between temperature variation and variation in lattice strain a/a_0 . Therefore one would predict that the incipient instability is the vanishing of G' , to occur at $(a/a_0)_{th} = 1.025$. From the simulation results at $T = 1350$ K (Fig. 4) one sees that the first structural response does have the predicted symmetry characteristics, and $(a/a_0)_{obs}$ is 1.024. This is an explicit confirmation that the vanishing of the tetragonal shear is responsible for the homogeneous melting of a defect-free crystal, as previously suggested [10]; also it signifies that the condition $G' = 0$ gives the upper limit of superheating or metastability [9,10] in this special case.

It is clear from Fig. 4(a) that the onset of the Born instability triggers both a shear [Fig. 4(b)] and lattice decohesion [Fig. 4(c)] instability, the latter showing a characteristic volume expansion. This behavior, which has not been recognized previously, implies that the signature of a first-order transition, namely, latent volume change, is not necessarily associated with the incipient instability. Thus, the picture of melting being driven by a thermoelastic instability [2], involving a combination of loss of shear rigidity [17] and vanishing of the compressibility [18], is correct *provided* it is applied to the phenomenon of mechanical instability of a crystal lattice and not to the coexistence of solid and liquid phases (melting in the thermodynamic sense) [7,10,12]. Furthermore, it appears that our simulation results showing explicitly the evolution of a sequence of elastic instabilities (cf. Figs. 2 and 4) lend support to the notion of a hierarchy of interrelated stability catastrophes of different origins [8].

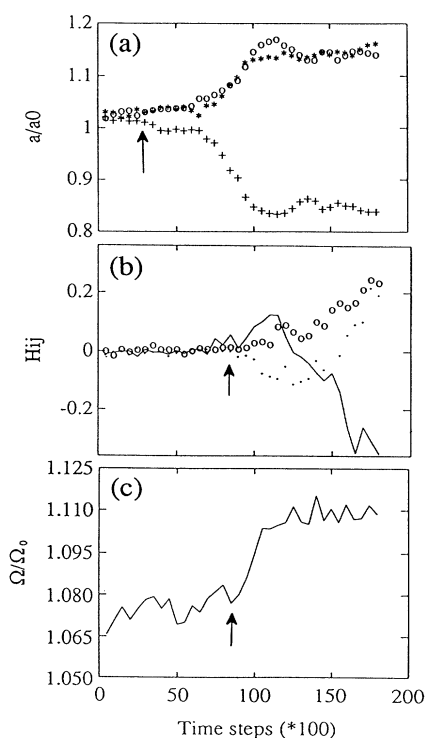


FIG. 4. Time response of (a) normalized lattice parameters along the three initially cubic directions, (b) matrix elements h_{12} , h_{13} , h_{23} , and (c) normalized system volume Ω/Ω_0 . Arrows indicate the onset of Born instability in (a), shear instability in (b), and lattice decohesion in (c).

Parallels between melting and crystal to amorphous transition have been discussed [9,10], where one may ask whether an elastic instability also can be the mechanism for homogeneous amorphization. In the case of α -quartz, stability criteria, expressed in terms of elastic stiffness coefficients derived from stress-strain relations, give a vanishing shear modulus in the correct pressure range where pressure-induced amorphization has been observed [19]. A fundamental question, still unresolved at present, is the role of elastic instability in solid-state amorphization when surface effects [10], point defects [20], or chemical disorder [9,21] have to be taken into account. The Born instability has been suggested as the trigger mechanism for amorphization in binary solid solutions [21]. To clarify this issue, it appears that extending the present stability analysis to include local deformation effects would be needed.

J.W. and S.Y. acknowledge helpful discussions with F.

A. McClintock. The work of J.W. and S.Y. has been supported in part by NSF (CHE-8806767), AFOSR (91-0285), ONR (N00014-92-J-1957), and the Materials Science Division, Argonne National Laboratory. J.W. also acknowledges a Graduate Fellowship award from the C. C. Wu Foundation. Work of S.R.P. and D.W. is supported by the U.S. Department of Energy, BES Materials Science, under Contract No. W-31-109-Eng-38. Computations were carried out in part under allocations from the San Diego Supercomputer Center and from the Lawrence Livermore National Laboratory.

*Present address: Materials Science Division, Argonne National Laboratory, Argonne, IL 60439.

- [1] M. Born and K. Huang, *Dynamical Theory of Crystal Lattices* (Clarendon, Oxford, 1956).
- [2] L. L. Boyer, *Phase Transitions* **5**, 1 (1985).
- [3] F. Milstein and B. Farber, *Phys. Rev. Lett.* **44**, 277 (1980).
- [4] J. S. Tse and D. D. Klug, *Phys. Rev. Lett.* **67**, 3559 (1991).
- [5] M. Parrinello and A. Rahman, *J. Appl. Phys.* **52**, 7182 (1981).
- [6] R. L. B. Selinger, R. M. Lynden-Bell, and W. M. Gelbart, *J. Chem. Phys.* **98**, 9808 (1993).
- [7] J. F. Lutsko, D. Wolf, S. R. Phillpot, and S. Yip, *Phys. Rev. B* **40**, 2841 (1989).
- [8] J. L. Tallon, *Nature (London)* **342**, 658 (1989).
- [9] W. L. Johnson, *Prog. Mater. Sci.* **30**, 81 (1986).
- [10] D. Wolf, P. R. Okamoto, S. Yip, J. F. Lutsko, and M. Kluge, *J. Mater. Res.* **5**, 286 (1990).
- [11] D. C. Wallace, *Thermodynamics of Crystals* (Wiley, New York, 1972).
- [12] J. Wang, S. Yip, S. R. Phillpot, and D. Wolf (to be published).
- [13] J. R. Ray, *Comput. Phys. Rep.* **8**, 109 (1988).
- [14] K. Huang, *Proc. R. Soc. London A* **203**, 178 (1950).
- [15] R. Hill and F. Milstein, *Phys. Rev. B* **15**, 3087 (1977).
- [16] S. M. Foiles, M. I. Baskes, and M. S. Daw, *Phys. Rev. B* **33**, 7983 (1986).
- [17] M. Born, *J. Chem. Phys.* **7**, 591 (1939).
- [18] K. Herzfeld and M. Goeppert-Mayer, *Phys. Rev.* **46**, 995 (1934).
- [19] N. Binggeli and J. R. Chelikowsky, *Phys. Rev. Lett.* **69**, 2220 (1992).
- [20] Y. Limoge, A. Rahman, H. Hsieh, and S. Yip, *J. Non-Cryst. Solids* **99**, 75 (1988); H. Hsieh and S. Yip, *Phys. Rev. Lett.* **59**, 2760 (1987).
- [21] M. Li and W. L. Johnson, *Phys. Rev. Lett.* **70**, 120 (1993).